Available online at www.sciencedirect.com

SCIENCE DIRECT

Biochimica et Biophysica Acta 1664 (2004) 182–188

BIOCHIMICA ET BIOPHYSICA ACTA BBA

www.bba-direct.com

Pore formation of phospholipid membranes by the action of two hemolytic arachnid peptides of different size

Olga S. Belokoneva[a], Honoo Satake[a], Elena L. Mal'tseva[b], Nadezhda P. Pal'mina[b], Elba Villegas[a,c], Terumi Nakajima[a], Gerardo Corzo[a,d,*]

[a] *Suntory Institute for Bioorganic Research, 1-1-1 Wakayamadai, Shimamoto-cho, Mishima-gun, Osaka 618-8503, Japan*
[b] *Institute of Biochemical Physics, Russian Academy of Sciences, Kosygina 4, Moscow, Russia*
[c] *Centro de Investigacion en Biotecnologia UAEM, Av. Universidad 2001, Cuernavaca, Morelos 62210, Mexico*
[d] *Institute of Biotechnology-UNAM, Av. Universidad 2001, Cuernavaca, Morelos 62210, Mexico*

Received 3 February 2004; received in revised form 18 May 2004; accepted 18 May 2004
Available online 11 June 2004

Abstract

Pin2 and Oxki1 are cationic amphipathic peptides that permeate lipid membranes through formation of pores. Their mechanism of binding to phosphocholine (PC) membranes differs. Spin-probe experiments showed that both Pin2 and Oxki1 penetrate the lipid membrane of small unilamellar vesicles (SUVs). Moreover, the leakage of calcein and dextrans from PC vesicles showed that Pin2 agrees with the accumulation of peptides on lipid membranes and form pores of different size. On the other hand, Oxki1 did not act strictly cooperatively and form pores of limited size.

Keywords: Cationic amphipathic peptide; Spider; Scorpion; FITC-dextran; Hemolysis; Antimicrobial

1. Introduction

Pore-forming peptides are linear cationic peptides with α-helical conformation broadly found in nature and induce permeation of lipid membranes [1,2]. It is presumed that pore formation of peptides in lipid layers is a time-dependent interaction [3] consisting of two major steps. The first step involves accumulation or oligomerization of peptides, which is suggestive of the critical ratio of peptide to lipid for induction of pore formation [3]. The second step is pore formation process itself, which is triggered by accumulation of peptides that have reached a critical density in the outer leaflet. The ''toroidal'' and ''barrel-stave'' models are the most accepted mechanisms of pore formation. In both mechanisms, the outer leaflet in membranes are carpeted with pore-forming peptides, followed by the integration of such peptides into the outer leaflet inducing a positive curvature strain. The surface area of the outer leaflet expands relative to the inner leaflet. Then, in the ''toroidal'' model, the membrane bends continuously from the top to the bottom in the fashion of toroidal hole. So, the peptides form a transmembrane pore, called toroidal pore, lined by both the peptide and lipids headgroups [3–8]. On the other hand, in the ''barrel-stave'' model, the α-helices of peptides are intercalated into lipids [9] where the peptides are unexceptionally associated with lipid headgroups even when they are perpendicularly inserted in the lipid bilayer [9,10]. In both models, the resultant pores cause leakage of lipid membrane contents such ions and small proteins. Melittin, magainin, and alamethicin have been the prototype peptides for the study of the mechanism of pore formation, and for the study of both the ''toroidal'' and the ''barrel-stave'' models. Those peptides are 20–26 amino acid residues long that aggregate in the outer leaflet membrane before inducing pore formation [11]. There are an increasing number of novel linear cationic

Abbreviations: PC, phosphatidylcholine; PE, phosphoethanolamine; SUV, small unilamellar vesicles; PBS, phosphate-buffered saline; Pin2, pandinin2; Oxki1, oxyopinin1; FITC, fluorescein isothiocyanate; 16DC, 16-doxyl-stearic acid

* Corresponding author. Institute of Biotechnology-UNAM, Av. Universidad 2001, Cuernavaca, Morelos 62210, Mexico. Tel.: +52-777-317-1209; fax: +52-777-317-2388.
E-mail address: corzo@ibt.unam.mx (G. Corzo).

0005-2736/$ - see front matter © 2004 Elsevier B.V. All rights reserved.
doi:10.1016/j.bbamem.2004.05.007

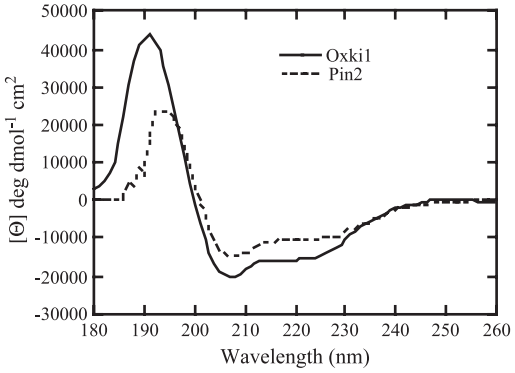

Fig. 1. Circular dichroism spectra of Oxki1 and Pin2. The secondary structures of Oxki1 and Pin2 were analyzed by circular dichroism spectrometry in 60% solution of TFE. The concentration of the peptides was 40 μg/ml. Data are the average of 10 separate recordings.

peptides whose size, hydrophobicity, and charge distribution are quite different from those of the prototype peptides, implying that the pore formation of membranes is a common overall mechanism but pore-forming peptides would have unique modes of insertion into the membrane surface.

Pandinin 2 (Pin2) and Oxyopinin 1 (Oxki1) are linear cationic peptides that have been isolated from the crude venoms of the scorpionid scorpion *Pandinus imperator* and of the oxyopid spider *Oxyopes kitabensis*, respectively [12,13] (Fig. 1). Pin2 and Oxki1 were shown to exert the inhibitory effects on the growth of both Gram-negative and positive bacteria and hemolytic activity on erythrocytes containing abundant phosphatidylcholine (PC) membranes [13,14]. The amino acid sequences of Pin2 and Oxki1 had similarities to that of molecules with pore-forming properties. Pin2 is 24 amino acid residues long and resembles the structure of Melittin (Table 1). Oxki1 is 48 amino acid residues long with low similarity to known pore-forming peptides; however, its N-terminal amino acid sequence (1–28) resembles the amino acid sequences of the transmembrane-spanning domains of some voltage-gated ion channels (Table 1). Other significant differences between Pin2 and Oxki1, besides their size, are their net charge and hydrophobicity (Table 1).

In this report, we focused on the pore-forming behavior of two arachnid peptides of different size. We found that Pin2 and Oxki1 bind differently to phosphocholine (PC) membranes, and based on dextran-loaded and spin-label experiments, they form membrane pores of different size through distinct binding mechanisms.

2. Materials and methods

2.1. Lipids and peptides

Egg L-α-phosphatidylcholine (PC) and calcein (fluorexone) were purchased from Nacalai Tesque Inc. (Kyoto, Japan). 1-Palmitoyl-2-hydroxy-*sn*-glycero-3-phosphocholine (LPC) was purchased from Avanti Polar Lipids, Inc. (USA). Sheep, pig, and Guinea pig erythrocytes were purchased from Nihon Seibutsu Zairyo Center (Osaka, Japan). Peptides Oxki1 and Pin2 were chemically synthesized by a solid phase method using the Fast-Fmoc methodology on an Applied Biosystems 433A peptide synthesizer according to previously published procedures [12].

2.2. Hemolytic assays

Hemolytic activity was determined by incubating a 10% (v/v) suspension of sheep, pig, or Guinea pig red blood cells with serial dilutions of each selected peptides. Red blood cells (10% v/v) were rinsed several times in PBS by centrifugation for 3 min at $3000 \times g$ until the OD of the supernatant reached the OD of the control (PBS only). Red blood cells were counted by a hemacytometer and adjusted to approximately $7.7 \times 10^6 \pm 0.37 \times 10^6$ cell/ml. Erythrocytes were then incubated at room temperature for 1 h in 10% Triton X-100 (positive control), in PBS (blank), or with the appropriate concentrations of peptide (0–30 μM). The samples were then centrifuged at $3000 \times g$ for 5 min; the supernatant was separated from the pellet and its absorbance measured at 570 nm. The blank supernatant absorbance was almost negligible, indicating the lack of spontaneous hemolysis during centrifugation. The relative OD compared to that of the suspension treated with 10% Triton X-100 defined the percentage of hemolysis.

2.3. Artificial vesicles

Small unilamellar vesicles (SUV) containing calcein were prepared according to Wieprecht et al. [15]. Calcein leakage from SUVs was monitored fluorometrically using a Hitachi Fluorescence Spectrophotometer F-4500 (Tokyo, Japan) by measuring the time-dependent increase in the fluorescence of calcein release. As calcein leaks from the SUVs due to the disrupting activity of the cationic peptides, it becomes diluted and therefore dequenched; the increase in fluorescence is recorded (excitation = 490 nm; emission = 520 nm). A final volume of 0.95 ml of the SUVs was placed in a stirred cuvette at room temperature. An aliquot of peptide solution (50 μl) was added to the cuvette. For LPC experiments, PC SUVs were preincubated for 2 min at room temperature including a sublytic concentration (1 μM) of LPC at 1 min. The percentage of calcein released by the addition of each peptide was evaluated by the equation: $100(F - F_o)/(F_t - F_o)$, where F is the fluorescence intensity achieved by the peptides, F_o is the fluorescence intensity observed without the peptides, and F_t is the fluorescence intensity corresponding to 100% calcein release determined by the addition of 50 μl of 10% Triton X-100. The phosphorus content in the phospholipid membranes was estimated by spectrophotometric analysis [16].

Table 1
Amino acid sequences and physical characteristics of Pin2 and Oxki1

Peptide	Peptide sequence	MW (Da)	Length (aa)	Mean hydrophobicity[a]	Net charge[b]
Pin2 (Melittin)	FWGALA**K**GAL**K**LIPSLFSSFS**KK**D GIGAVL**K**VLTTGLPALISWI**KRKR**QQ	2612.1	24	0.560	+3
Oxki1 (IVS4)[c]	F**R**GLA**K**LL**K**IGL**K**SFA**R**VL**KK**VLP**K**AA**K**AG**K**ALA**K**SMADENAI**R**QQNQ F**R**VI-**R**LA**R**IG-**R**IL-**R**LI**K**GA- -**K**GI**R**	5221.3	48	−1.580	+10

[a] Hydrophobicity was calculated using HydroMcalc by Sandri L. (http://www.bbcm.univ.Triestreittossi/Hydrocalc/HydroMCalc.html) on the basis of CCS, a corrected hydrophobicity scale derived from two consensus scales; the GCS scale is based on 160 scales found in the literature and the XCS scale is based only on 33 strictly experimental hydrophobicity scales.

[b] The peptide net charge was calculated under the assumption that at physiological conditions Lys, Arg, and the N-termini are positively charged, and Glu, Asp, and C-terminals are negatively charged.

[c] Putatitive S4-charged membrane-spanning domain from domain IV of the Nav 1.2 voltage-gated ion channel.

2.4. Surface plasmon resonance experiments

The interactions of the zwitterionic peptides with PC layers were assessed using a biosensor instrument, SPR-CelliA (Nippon Laser and Electronics, Nagoya, Japan). Gold-coated sensor chips (Nippon Laser and Electronics) were incubated in 10 mM 1-octadecanethiol in ethanol overnight at room temperature, and rinsed with ethanol three times. The 1-octadecanethiol-associated chip was mounted on a detector of the SPR instrument, washed by injection of 40 mM octyl-glicoside (25μl), and equilibrated with a running buffer (20 mM phosphate buffer, pH 6.8) at flow rate of 5 μl/min. Thirty microliters of PC membrane suspension (0.5 mM) as prepared above was applied to the sensor chip at 2 μl/min. Excess PC was removed by application of 30 μl sodium hydroxide (10 mM) at 50 μl/min. After the stable baseline was observed, each peptide solution at various concentrations was injected at 5 μl/min, and the kinetics of binding was monitored. All observations were performed at 25 °C. All biochemical parameters were calculated by SPR analysis software (Nippon Laser and Electronics).

2.5. Preparation of dextran-loaded liposomes and leakage experiments

Fluorescein isothiocyanate (FITC)-labeled dextrans (FDs) (Sigma Co., USA) with different molecular weights (kDa) and radii (nm) were used; FD4 (3.9 kDa, 1.8 nm [17]), FD20 (19.8 kDa, 3.3 nm [18]), FD40 (40.5 kDa, 4.8 nm [18]) and FD70 (71.6 kDa, 5 nm [17]) were utilized as model cytoplasmic components. Dextran-loaded PC liposomes (bilayered/multilayered phospholipids) containing the fluorescein isocyanate were prepared as reported by Rinaldi et al. [19]. A buffer solution (1 ml, 50 mM potassium phosphate, pH 7.4, with 0.1 mM EDTA) containing 2 mg/ml of the dextran of choice was sonicated with a PC solution in chloroform (20 mg/ml) for 30 min on ice. Chloroform was evaporated using a rotary vacuum evaporator (Tokyo Rikaki, Tokyo, Japan) at room temperature. As the solvent was progressive removed, the material first formed a viscous gel, and, subsequently, it formed a liposome suspension. At this point, 2 ml of buffer was added, and the suspension was evaporated for an additional hour to remove eventual traces of chloroform [20]. After the formation of liposomes, untrapped dextran was removed by several cycles of centrifugation (22,000 × *g* for 30 min) and washed with potassium phosphate buffer, until the residual fluorescence in supernatant was negligible. For experiments, an aliquot of peptide solution was incubated with a suspension of dextran-loaded liposomes. The mixture (2 ml, final volume) was stirred for 10 min in the dark and then centrifuged at 22,000 × *g* for 30 min. The supernatant was recovered and its fluorescence intensity recorded. Excitation and emission wavelengths were 494 and 520 nm, respectively. Positive controls and maximum fluorescence intensity corresponding to 100% leakage were determined by adding 20 μl of 10% Triton X-100 to the liposome suspension.

2.6. Spin probes experiments

Microviscosity studies of PC SUVs has been studied by electron paramagnetic method (EPR) applicable to lipid bilayer structure using the spin probe 16-doxyl-stearic acid (16DC) [21,22]. Egg L-α-phosphatidylcholine (PC) was used to prepare SUVs. Aliquots of chloroform/methanol solution of PC, and 16DC were combined to give the PC/spin label mole ratio of 60:1. SUVs were prepared with 4 ml solution of PC:16DC evaporated in vacuum and added 4 ml of buffer A (10 Tris−HCl, 2 mM EDTA, 150 mM NaCl, pH 7.0). The mixture was sonicated at 100 V for 15 min, and then, centrifuged at 13,000 × *g* for 10 min. The supernatant containing multilamellar PC:16DC SUVs was used for spin probe experiments. Peptide aliquots of Pin2 and Oxki1 were prepared in acetonitrile/H_2O (1:1), vacuum dried, and then resuspended in PC:16DC SUVs. EPR spectra were obtained by Brucker-200D spectrometer (Germany) to estimate a value of rotational correlation time (τ) for fast motion range of rotational rates ($\tau < 10^{-9}$s) [23]; $\tau = 6.65\ \Delta h_{+1}/[(I_{+1}/I_{-1})^{1/2} - 1] \times 10^{-10}$ s, where I_{+1} and I_{-1} are the resonance heights of low- and high-field components of EPR spectra, respectively; Δh_{+1} is the resonance width of the high-field components. Δh_{+1} was calculated by subtracting the value for the lipid alone from that of the lipid−peptide sample. Curves of τ (%) variation

$[(\tau_o - \tau) \times 100/\tau_o]$ for the 16DC probe in the PC SUVs as a function of peptide concentration of each arachnid peptide were obtained.

3. Results

3.1. Distinct permeation and binding of biological and artificial membranes

Pin2 has a higher propensity to lyse pig erythrocytes than Oxki1 (Fig. 2A). The hemolysis assay of Pin2 showed an exponential dose–response curve, indicating that toxin aggregation or oligomerization might be required for pore formation. Similar results were observed in artificial PC SUVs (Fig. 2B). The addition of Pin2 to calcein-loaded PC SUVs caused dye efflux at low peptide concentration in a sigmoidal dose–response manner. Compared to Pin2, a larger amount (fivefold) of Oxki1 was required to induce a similar extent of calcein release, but the dose–response curve of Oxki1 was nonsigmoidal entirely, suggesting a different mechanism of pore formation to that of Pin2. Kinetic analyses of calcein leakage produced by Pin2 and Oxki1 were performed and initial rates of leakage were calculated from the initial linear time variation of the fluorescence intensity of experimental traces. Only in the case of Pin2, a sigmoidal shaped curve was clearly observed (Fig. 2C), suggesting again that calcein leakage could be related to a membrane disruption process depending on interactions between protein monomers of this peptide. To further analyze the possibility of peptide oligomerization, the reaction order of calcein release were calculated from double logarithmic plots of the initial rates vs. peptide-to-lipid ratios (Fig. 2C, inset). Values of 2.7 and 1.5 were obtained for Pin2 and Oxki1, respectively.

Melittin, a well-known peptide for its pore-forming ability, was used as a positive control to compare the binding properties of Oxki1 and Pin2. Kinetic parameters determined from SPR observation indicated that Oxki1 binds to PC layers to a similar degree to melittin. This result supported the notion that Oxki1 possesses a membrane affinity typical to amphiphilic peptides such as melittin (Table 2). However, we failed to assess the binding of Pin2 to PC layers, given that Pin2 showed unusual binding curves, which was not applicable for the quantitative SPR analysis. These results showed the distinct binding properties between Oxki1 and Pin2.

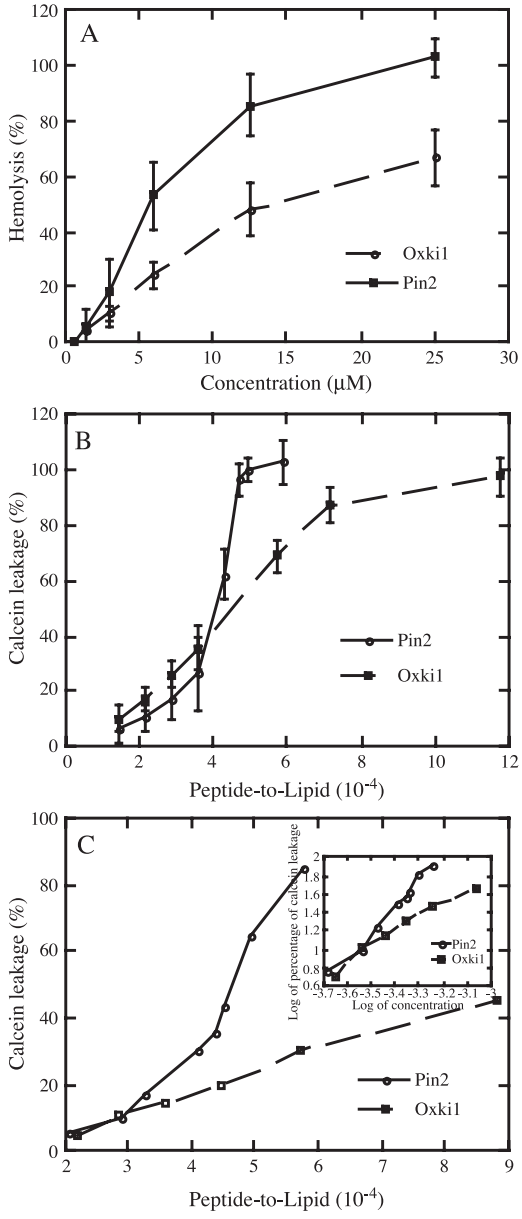

Fig. 2. Membrane-disrupting activities of Pin2 and Oxki1. (A) Pig red blood cells. The values represent the average mean ± S.D. of three independent experiments. A positive control was determined using a 10% solution of Triton X-100. (B) PC SUVs. The lipid concentration employed was 84 μM. Percent of leakage is plotted as a function of peptide to lipid ratio. Mean ± S.D. of two independent experiments. (C) Initial rates of calcein leakage produced during the first 10 s after application of peptides. The inset figure corresponds to the double-logarithmic plot of the values in C. The total lipid concentration employed was 73 μM. Values are average of five and seven experiments for Pin2 and Oxki1, respectively.

3.2. Membrane curvature experiments

The effects of the membrane curvature on the pore formation by Oxki1 and Pin2 were investigated by observation of the pore-forming mode in egg yolk PC calcein-loaded SUVs treated with phosphatidylethanolamine (PE). As shown in Fig. 3A, the incorporation of PE into the PC calcein-loaded SUVs (1:1) did not significantly change the Pin2-induced leakage of calcein from PC/PE SUVs. On the other hand, the incorporation of PE significantly inhibited the Oxki1-induced calcein release of PC/PE SUVs (Fig. 3A). Moreover, incorporation of 1-oleoyl-2-hydroxy-*sn*-glycero-3-phosphocholine (LPC), a cone-shaped phospholipid that induces positive curvature of the calcein-loaded PC lipid bilayers, significantly sensitized calcein release by Oxki1 (Fig. 3B), but did not alter calcein release by Pin2

Table 2
Binding constants of Melittin and Oxyopinin 1 to PC layers

Peptide	K_D (M)	K_{ass} (1/M)	K_{aff} (1/M s)	K_{dis} (1/s)
Melittin	1.8×10^{-5}	5.5×10^{4}	291.3	6.6×10^{-3}
Oxki1	5.6×10^{-5}	1.7×10^{4}	79.6	4.4×10^{-3}

Values are means of two independent measurements.

(not shown). These results demonstrated that membrane curvature influence pore formation induced by Oxki1 while it will not affect that of Pin2.

3.3. The effect of Pin2 and Oxki1 on fatty acid spin label in SUVs

Curves of τ (%) variation $[(\tau_o - \tau)100/\tau_o]$ for 16DC probe in the PC SUVs as a function of peptide concentration for Pin2 and Oxki1 were obtained (Fig. 4). The τ variation

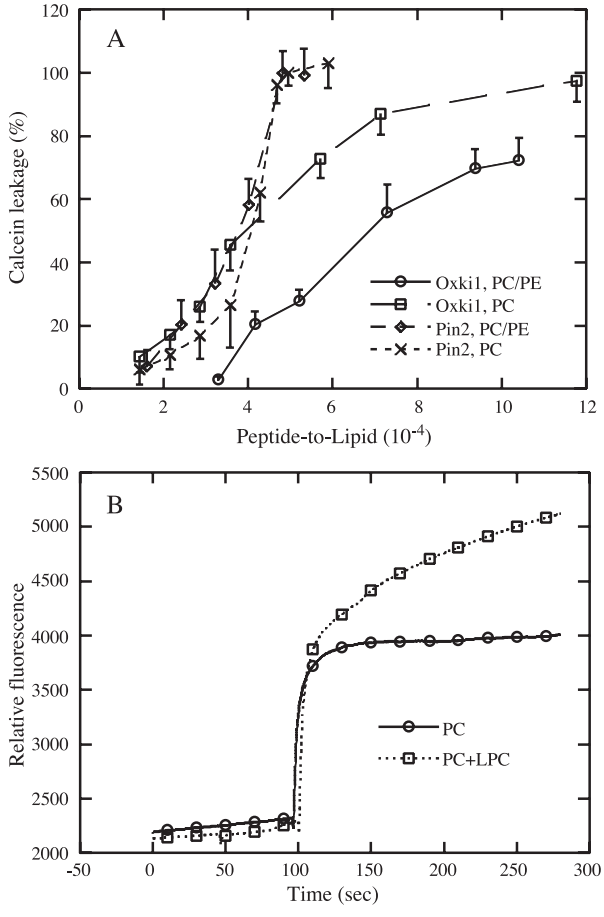

Fig. 3. Effect of PE and LPC incorporation on PC SUVs. (A) PE incorporation to PC SUVs. Values are the mean ± S.D. of three independent experiments. (B) Effect of LPC on Oxki1-induced calcein release. Calcein-loaded PC SUVs were injected at time zero into the buffer preincubated at room temperature. The final lipid concentration was 84 μM. Fluorescence intensity was continuously monitored at 520 nm (excitation at 490 nm). Addition of Oxki1 (15 nM) at 2 min induced dye release, resulting in fluorescence increase (solid trace). In the case of the dashed trace, sublytic concentration of LPC (1 μM) was pretreated at 1 min. The Oxki1-triggered calcein leakage was significantly sensitized.

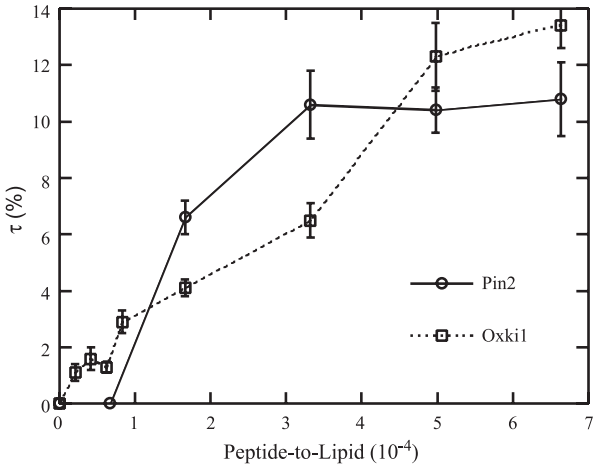

Fig. 4. Percentage of τ variation of spin label 16-DC in PC SUVs. (A) Pin2 and (B) Oxki1. Mean ± S.D. of two independent experiments.

for both peptides increased up to 12% (the saturation level), indicating decreased motional frequency of the probe. The motional frequency decreased with increase of P/L ratio for

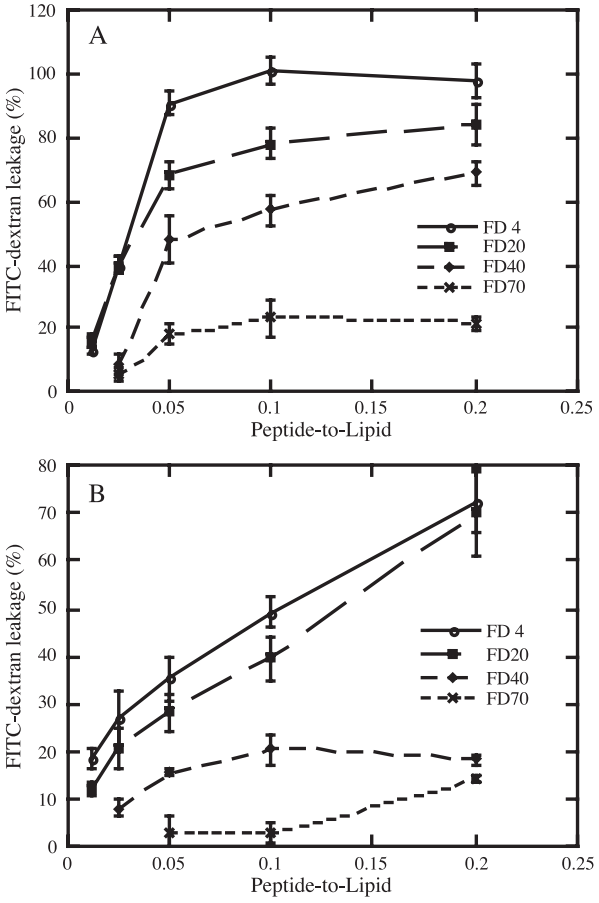

Fig. 5. FITC-dextran release from PC liposomes. (A) Pin2 and (B) Oxki1. PC liposomes (50 μM) containing FITC-dextrans of FD4, FD20, FD40, or FD70 were incubated in the presence of different concentrations of the peptides for 10 min at room temperature. Values are the mean ± S.D. of three independent measurements.

both peptides. The experimental dose-dependence curve for Pin2 displayed a sigmoidal curve with the increase of peptide-to-lipid ratio. On the other hand, Oxki1 increased the τ variation parameter in a linear fashion.

3.4. Permeation of dextran-loaded PC liposomes

To estimate the size of the membrane defects caused by Oxki1 and Pin2, the release of FITC-dextrans from PC liposomes was investigated. Pin2 exhibits a strong size dependence in the release of encapsulated markers at concentrations up to 10 μM (Fig. 5A). The FD4 release from PC liposomes at 10 μM (P/L = 0.2) of Pin2 attained 90%, whereas the FD70 leakage was only 15%. There were significant differences in the leakage of FD4, FD20, FD40, or FD70 liposomes at all range of Pin2 concentrations. The results obtained with Oxki1 revealed also a size dependence in the release of the fluorescent markers by Oxki1 (Fig. 5B). In particular, Oxki1 was found to release 50% of FD4 but only 6% of FD70 from PC liposomes at a peptide concentration of 5 μM (P/L = 0.1).

4. Discussion

4.1. Pin2 and Oxki1 affect permeation of biological and artificial membranes

Because the number of amino acid residues of Oxki1 is 48 and that of Pin2 is 24, the length of Oxki1 and Pin2 are expected to be 36 and 72 Å (1.5 Å per residue), respectively. Therefore, they are large enough to span biological and artificial membranes; and thus, to form of pore-like structures. The shape of the hemolysis and calcein leakage of the dose–response curves suggested that the mechanism of permeation of Pin2 differs from that of Oxki1. Contrary to Oxki1, curves for Pin2 were sigmoidal, suggesting an accumulation of peptides in the membrane before pore formation. Accumulation of peptides are often observed in antimicrobial peptides such melittin, magainin, and alamethicin whose size is similar to that of Pin2. Furthermore, the membrane-disrupting kinetics of Pin2 and Oxki1 as well as the reaction order of 2.7 and 1.5, respectively, suggest that Pin2 molecules cooperate largely than that of Oxki1 to induce membrane leakage.

4.2. Membrane curvature influence disrupting activity of Oxki1 but not of Pin2

Pore-forming peptides are greatly affected by the membrane curvature, and their mode of action could be understood by the manner how they alter the intrinsic curvature properties of lipid bilayers. For example, peptides that promote negative curvature are more potent for pore formation than peptides that impose positive curvatures [24,25]. Pin2 was not affected by curvature stress; however, positive curvature favored pore formation by Oxki1. For instance, positive curvature stress on lipid membranes caused by magainin2 leads to the formation of toroidal pores [4,5], and the incorporation of PE, which induce negative curvature, to PG-based bilayers inhibited magainin-induced pore formation [26]. Because membrane positive curvature favors pore formation and membrane negative curvature diminishes pore formation by Oxki1, this peptide is more likely to form toroidal pores. This hypothesis is reinforced by the fact that the pore size observed during permeation of dextran-loaded PC liposomes by Oxki1, as well as in magainin, had a limited size [27]. Contrary to Oxki1, Pin2 was not affected by membrane curvature and it created pores of different size; however, this behavior does not exclude Pin2 of forming toroidal pores.

4.3. The effect of Pin2 and Oxki1 on fatty acid spin label in PC SUVs

It was shown that the membrane-spanning and pore forming peptide melittin has a great effect on acyl chain organization, leading to a marked decrease in membrane fluidity [28]. Pin2 and Oxki1 increase the fatty acid chain order, or in other words, restrict the motion of the lipid chains in SUVs. Therefore, Pin2 and Oxki1 seem to penetrate toward the hydrocarbon core of the membrane indicating pore-forming mechanisms. Thus, in PC SUVs Oxki1 and Pin2 affected the lipid acyl chains at the submersion level about 20 Å (16DC). Moreover, there was a full correspondence in the curves of dose-response between membrane disrupting effects (calcein leakage) and restriction of the motion of lipid chains of 16DC.

4.4. Permeation of dextran-loaded PC liposomes

Pores created by Pin2 and Oxki1 could pass calcein (623 Da) freely. However, clear size-restricted leakage of encapsulated markers by Oxki1 and Pin2 was observed by the permeation analyses using FITC-labeled dextrans with various radii (Fig. 5). The hydrodynamic radii for FD4 and FD70 are estimated to be 1.8 and 5 nm, respectively [17]. Oxki1 allowed the leakage of FD4 and FD10 but significantly restricted the passage of FD40 and FD70, providing evidence that Oxki1 forms pore with inner radius lower than 1.8 nm at peptide–lipid ratios from 0.02 to 0.1. On the other hand, Pin2 allowed a size dependence leakage of FD4, FD20, and 50% of FD40. Therefore, the pore size radii induced by Pin2 could expand from 1.8 to 5 nm in a peptide–lipid ratio-dependent manner. The leakage of a small percentage (>20%) of FD40 and FD70 in the presence of Oxki1 and that of FD70 in the presence of Pin2 were most likely due to the molecular configuration of dextrans. Dextrans are best modeled as prolate ellipsoids and some minor leakage could result from restricted passage through the pore by reptation as pointed out by Ladokhin et al. [29].

5. Conclusions

This work shows that Pin2 and Oxki1 permeate lipid membranes through formation of pores, and their mechanism and size of pore differ in each other. The sigmoidal behavior of Pin2 agrees with the accumulation of peptides on lipid membranes where the cooperative of monomers could trigger the formation of pores in a similar way to magainin, alamethicin, and other pore-forming peptides of similar size. The formation of pores of different size depending on the peptide-to-lipid ratio by Pin2 resembles that of Melittin [30] except for the SPR analysis that showed different binding behavior to PC. On the other hand, Oxki1 did not act strictly cooperatively, i.e., it does not follow the carpeting of lipid membranes and it seems to form pores of limited size. These results suggest that Oxki1 forms pores following different mechanism to that of Pin2. Although these possible molecular mechanisms are speculative, they are based on data of different phenomenological experiments. The binding action of Pin2 and the low cooperation of Oxki1 molecules may grant further studies of pore formation.

Acknowledgements

This work was supported in part by a grant from the Research for the Future Program from the Japanese Society for the Promotion of Science (JSPS).

References

[1] W.L. Maloy, U.P. Kari, Structure–activity studies on magainins and other host defense peptides, Biopolymers 37 (1995) 105–122.
[2] D. Andreu, L. Rivas, Animal antimicrobial peptides: an overview, Biopolymers 47 (1998) 415–433.
[3] K. Matsuzaki, Why and how are peptide–lipid interactions utilized for self-defense? Magainins and tachyplesins as archetypes, Biochim. Biophys. Acta 1462 (1999) 1–10.
[4] K. Matsuzaki, O. Murase, N. Fujii, K. Miyajima, An antimicrobial peptide, magainin 2, induced rapid flip-flop of phospholipids couple with pore formation and peptide translocation, Biochemistry 35 (1996) 11361–11368.
[5] S. Ludtke, K. He, W.T. Heller, T.A. Harroun, L. Yang, H.W. Huang, Membrane pores induced by magainin, Biochemistry 35 (1996) 13723–13728.
[6] K. He, S.J. Ludtke, H.W. Huang, D.L. Worcester, Antimicrobial peptide pores in membranes detected by neutron in-plane scattering, Biochemistry 34 (1995) 15614–15618.
[7] L. Yang, T.A. Harroun, T.M. Weiss, L. Ding, H.W. Huang, Barrel-stave model or toroidal model? A case study on melittin pores, Biophys. J. 81 (2001) 1475–1485.
[8] M. Zasloff, Antimicrobial peptides of multicellular organisms, Nature 415 (2002) 389–395.
[9] M.S. Sansom, The biophysics of peptide models of ion channels, Prog. Biophys. Mol. Biol. 55 (1991) 139–235.
[10] K. He, S.J. Ludtke, D.L. Worcester, H.W. Huang, Neutron scattering in the plane of membranes: structure of alamethicin pores, Biophys. J. 70 (1996) 2659–2666.
[11] H.W. Huang, Action of antimicrobial peptides: two-state model, Biochemistry 39 (2000) 8347–8352.
[12] G. Corzo, P. Escoubas, E. Villegas, K.J. Barnham, W. He, R.S. Norton, T. Nakajima, Characterization of unique amphipathic antimicrobial peptides from venom of the scorpion *Pandinus imperator*, Biochem. J. 359 (2001) 35–45.
[13] G. Corzo, E. Villegas, F. Gomez-Lagunas, L.D. Possani, O.S. Belokoneva, T. Nakajima, Oxyopinins, large amphipathic peptides isolated from the venom of the wolf spider *Oxyopes kitabensis* with cytolytic properties and positive insecticidal cooperativity with spider neurotoxins, J. Biol. Chem. 277 (2002) 23627–23637.
[14] O.S. Belokoneva, E. Villegas, G. Corzo, L. Dai, T. Nakajima, The hemolytic activity of six arachnid cationic peptides is affected by the phosphatidylcholine-to-sphingomyelin ratio in lipid bilayers, Biochim. Biophys. Acta 1617 (2003) 22–30.
[15] T. Wieprecht, O. Apostolov, J. Seelig, Binding of the antibacterial peptide magainin 2 amide to small and large unilamellar vesicles, Biophys. Chem. 85 (2000) 187–198.
[16] C.J.F. Böttcher, C.M. Van Gent, C. Fries, A rapid and sensitive submicro phosphorus determination, Anal. Chim. Acta 24 (1961) 203–204.
[17] M.P. Bohrer, W.M. Deen, C.R. Robertson, J.L. Troy, B.M. Brenner, Influence of molecular configuration on the passage of macromolecules across the glomerular capillary wall, J. Gen. Physiol. 74 (1979) 583–593.
[18] T.C. Laurent, K.A. Granath, Fractionation of dextran and Ficoll by chromatography on Sephadex G-200, Biochim. Biophys. Acta 136 (1967) 191–198.
[19] A.C. Rinaldi, A. Di Giulio, M. Liberi, G. Gualtieri, A. Oratore, A. Bozzi, M.E. Schinina, M. Simmaco, Effects of temporins on molecular dynamics and membrane permeabilization in lipid vesicles, J. Pept. Res. 58 (2001) 213–220.
[20] F. Szoka Jr., D. Papahadjopoulos, Procedure for preparation of liposomes with large internal aqueous space and high capture by reverse-phase evaporation, Proc. Natl. Acad. Sci. U. S. A. 75 (1978) 4194–4198.
[21] P.C. Jost, O.H. Griffith, in: L.J. Berliner (Ed.), Lipid Spin Labels in Biological Membranes, Academic Press, New York, 1976, pp. 453–523.
[22] P. Jost, L.J. Libertini, V.C. Hebert, O.H. Griffith, Lipid spin labels in lecithin multilayers. A study of motion along fatty acid chains, J. Mol. Biol. 59 (1971) 77–98.
[23] A.N. Kuznetsov, Spin Label Method, Nauka, Moscow, 1976.
[24] R.F. Epand, R.M. Epand, V. Monaco, S. Stoia, F. Formaggio, M. Crisma, C. Toniolo, The antimicrobial peptide trichogin and its interaction with phospholipid membranes, Eur. J. Biochem. 266 (1999) 1021–1028.
[25] D.P. Siegel, R.M. Epand, The mechanism of lamellar-to-inverted hexagonal phase transitions in phosphatidylethanolamine: implications for membrane fusion mechanisms, Biophys. J. 73 (1997) 3089–3111.
[26] K. Matsuzaki, K. Sugishita, N. Ishibe, M. Ueha, S. Nakata, K. Miyajima, R.M. Epand, Relationship of membrane curvature to the formation of pores by magainin 2, Biochemistry 37 (1998) 11856–11863.
[27] T. Tachi, R.F. Epand, R.M. Epand, K. Matsuzaki, Position-dependent hydrophobicity of the antimicrobial magainin peptide affects the mode of peptide–lipid interactions and selective toxicity, Biochemistry 41 (2002) 10723–10731.
[28] J.E. Mahaney, D.D. Thomas, Effects of melittin on molecular dynamics and Ca-ATPase activity in sarcoplasmic reticulum membranes: electron paramagnetic resonance, Biochemistry 30 (1991) 7171–7180.
[29] A.S. Ladokhin, M.E. Selsted, S.H. White, Sizing membrane pores in lipid vesicles by leakage of co-encapsulated markers: pore formation by melittin, Biophys. J. 72 (1997) 1762–1766.
[30] N. Papo, Y. Shai, Exploring peptide membrane interaction using surface plasmon resonance: differentiation between pore formation versus membrane disruption by lytic peptides, Biochemistry 42 (2003) 458–466.